

Mechanical, morphological and water absorption properties of polyethylene/olive pomace flour bio-composites

Raid Banat*, Malek Aljnaid, Manal Al-Rawashdeh

Department of Chemistry, Al al-Bayt University, P.O.BOX 130040, Mafrqa, 25113, Jordan

Received: 11 May 2021, Accepted: 11 July 2021

ABSTRACT

Mechanical and physical properties of various weigh percentages (0% - 40%) of olive pomace flour (OPF)-loaded linear low density polyethylene (LLDPE) in the presence of 0%, 5% and 10% coupling agent (C) were formulated and studied. Extrusion and hot press processing techniques were used to fabricate OPF/LLDPE composites. Tensile stress at yield increased by 20% with the increasing of the filler loading up to 20%; and marginally increased in the presence of the C. Whereas, the decline in the tensile strain at yield of the polymer composite improved with the increase in the C content. The modulus increased from 631 MPa for the neat LLDPE to 680, 808 and 700 MPa for the composites filled by 5%, 10% and 20% filler content, respectively. Whereas, a decrease in the given modulus (550 MPa) was observed at 40% filler loading. The modulus has shown a successive improvement upon the addition of the C with values not less than 800 MPa. The impact strength decreased with the increase in filler loading from 119 kJ/m² for the neat LLDPE to 81, 43, 27 and 16 kJ/m² for the 5%, 10%, 20% and 40% OPF/LLDPE samples, respectively. On the contrary, 10% C addition improved the impact strength of the composite by two folds in the case of 10 - 40% filler inclusion. The scanning electron microscopy (SEM) illustrations proved the mechanical performance of various bio-composite formulations. Water absorption of the bio-composite increased with the OPF loading, from 0.73% for the neat LLDPE to 2.6% for 40% OPF-filled polymer composite, and decreased upon increasing the C content with an average of 1.4% for all composites. Formulated by mixing cellulosic-based material OPF and LLDPE, the bio-composite demonstrated compatible physical properties and can be used as an already available cellulosic filler for the bio-composite materials. **Polyolefins J (2022) 9: 1-14**

Keywords: Olive pomace flour; LLDPE; coupling agent; bio-composite; mechanical and physical properties.

INTRODUCTION

Lignocellulosic fiber is a biorenewable natural fiber. Low cost, recyclability, and biodegradability of lignocellulosic material are among many other advantages, making it a good candidate in bio-composite manufacturing [1-3]. Flax, sisal, pine, hemp and other lignocellulosic fibers are already known fillers in product manufacturing based on green materials [4-6]. Agro waste is considered as a resource of the natural fiber in

producing the bio-composite material [7-9]. Lignocellulosic-based polymer bio-composite suffers from their sensitivity towards the moisture and water environment that affected the whole performance of the material [10-12]. Interfacial adhesion and poor chemical resistance are also considered as the drawbacks of such lignocellulosic-based polymeric bio-composite materials [13-15]. Residues and by-products from the agricultural

*Corresponding Author - E-mail: raidbanat@aabu.edu.jo

crops can aid as a source for power and developing new bio-composite formulation [16-18]. Efforts on reducing the negative impact of agro wastes on the environment have increasingly developed in the recent years [19-21]. Nowadays, processed agro waste is considered as a competitive raw material in various applications. For example, such material is used as a filler in reinforcing thermoplastic polymers [22-25]. Minimizing version polymer production and consumption [26, 27], emerging new recycled material, reducing wastes, manufacturing biodegradable products [28, 29] and functioning clean technologies are of the main concerns of states regulations that guide industry and researchers in the recent decade.

Nanocomposites from corn starch/modified clay films were prepared and studied. The antibacterial activity was enhanced and the mechanical performance was also increased due to the inclusion of the silver metal ion modified zinc and copper-based clay nanoparticle material [30, 31]. The developed starch/nanoclay films are considered as a potential candidate for use in food packaging application [32]. Similar results were obtained when nanoparticles of silver, copper oxide, and zinc oxide were incorporated separately into both matrix of low-density polyethylene and carboxymethyl cellulose to prepare active packaging films [33, 34].

Lignocellulosic solid waste, which is generated from the olive oil extraction process, is approximately representing 35% of the whole olive fruit [35, 36]. Wastes from olive oil production were considered as a serious environmental threat. A few decades ago olive solid waste was used as a source of the thermal energy by direct combustion. Later, over the past decade, researchers performed various approaches to utilize olive oil residue as a filler material in polymers [37-39]. Promising bio-composite material based on the mentioned waste is developed and produced for some polymeric materials. The use of the olive pomace (OP) as a plastic filler was partially covered by some researchers for certain types of polymers. OPF as a filler material still needs further investigation using other types of polymer matrices. Chemically modified polymer additives, to reduce interfacial tension at the polymer/filler boundaries, have shown successive development on the commercial scale. Utilization of

OPF as filler in several polymeric matrices was introduced by many authors [40]. Polymer matrices such as polylactic acid (PLA) [41-43], polypropylene (PP) [44-46], polyvinyl chloride (PVC) [47], saturated and unsaturated polyester [48, 49], epoxy resins [50-51], chitosan [52-53], wheat gluten [54] and high density polyethylene (HDPE) [55, 56] were studied and reported. However, a lack of research on the utility of other types of polymer materials is apparent and needs more investigation. In this research, a bio-composite material which contains OPF mixed with LLDPE was formulated and investigated. The aim of this study was to launch OPF/LLDPE bio-composite and to investigate the effect of the natural filler loading on its physical and mechanical properties. Marketable C (Dow Chemical) was also used to assess its effect on the filler/polymer interfacial adhesion.

EXPERIMENTAL

Materials

The homopolymer, LLDPE (SABIC® LLDPE M500026), was used as the polymer matrix in the composite material. This LLDPE has a narrow molecular weight distribution with excellent flow properties, as well as it is low temperature toughness grade and with a melt flow index of 50 g/10 min. The coupling agent (C) used in this study is under a trade name of Fusabond® E 226 resin, which is an anhydride modified polyethylene, with 0.93 g/cm³ density, 120°C melting point and 290°C maximum processing temperature, was kindly provided by Dupont Company. The present modifier resin (C) is used to improve the surface adhesion between the wood filler/polymer matrix phases. Olive pomace was obtained from a local olive press plant and used as a filler after some conditioning.

Methods

OPF Preparation

Residues of olive oil production process known as olive pomace were obtained from the local press plant. After olive oil extraction, the remaining skin, pulp, and stone were the main components of the residue. The obtained olive pomace was used without any chemical modifications and dried at 105°C for 24 h.

The resulting olive pomace was ground into the fine flour. A Pulverisette 9 vibrating cub mill (Fritsch, Germany) was used to grind OP, where the particle mesh size was measured with a set of sieves with 70 mesh. Filler was dried in an oven at 105°C for 24 h to adjust moisture.

Composite Processing

Prior to extrusion process, LLDPE and OPF were dried at 105°C for 24 h. Polymer, filler and coupling agent were mixed by using a twin screw extruder (TSE 20, L/D: 40:1, diameter 22 mm) with the working temperature range of 165°C - 185°C. The operating screw speed and feed rate were 50 rpm and 1.5 kg/h, respectively. Extruded LLDPE/OPF samples were then compression molded using a digital hot (XH-406B) press at 150°C.

The compression time was set at 30 s. Bio-composites with OPF and C content varied from 0% to 40 % and from 0% to 10%, respectively. The weight percentage of each component in bio-composite material is summarized in Table 1. Aluminum molds were used to prepare sample sheets in a compression-molding machine (XH-406B). Polymer bio-composite with predetermined formulation was compression molded in the form of sheets with dimensions of 30 × 20 × 2 mm. Standard dog-bone specimens were sliced from OPF/LLDPE sheet to carry out mechanical tensile test in agreement with ASTM D-638/IV type. The impact strength test samples were shaped in an aluminum mold with standard dimensions of 63.5 × 6.4 × 12.7 mm.

Table 1. Formulation of the composites.

Sample No.	Sample ID	Weight Percent (%)		
		LLDPE	OPF	Coupling Agent
1	100P+0F+0C	100	0	0
2	95P+5F+0C	95	5	0
3	90P+5F+5C	90	5	5
4	85P+5F+10C	85	5	10
5	90P+10F+0C	90	10	0
6	85P+10F+5C	85	10	5
7	80P+10F+10C	80	10	10
8	80P+20F+0C	80	20	0
9	75P+20F+5C	75	20	5
10	70P+20F+10C	70	20	10
11	60P+40F+0C	60	40	0
12	55P+40F+5C	55	40	5
13	50P+40F+10C	50	40	10

Bulk Density

The bulk density of the dried OPF (80°C for 24 h) was determined by using a high precision graduated cylinder to measure the volume of exactly 50 g of OPF filler.

Moisture Content

10 g OPF samples with a mesh size of less than 70 were placed in an aluminum dish, weighted and then dried in an oven at 103 ± 2°C for 48 h. Moisture content was determined using Eqn (1):

$$\text{Moisture content(\%)} = [(Wt_w - Wt_o) / Wt_o] \times 100 \quad (1)$$

where, Wt_w is the weight of the wet sample and Wt_o is the weight of the oven dried one.

Mechanical Analysis

The OPF-filled LLDPE samples were put down at 25°C and 15 % humidity for 48 h. Dog-bone shaped specimens were prepared according to ISO 180 test standard. Afterwards, a WDW-5 brand computer control electrical universal testing machine, operating at a rate of 2 mm/min, was used to evaluate and analyze the tensile strength and the Young's modulus of the polymer composite. Izod impact strength of the un-notched specimens was measured as stated in the ASTM: D256 utilizing an FI-68 impact testing machine of 3.5 m/s impact speed, and 2.270 kg hammer's weight. The mean value of at least 7 samples was reported for each composite formulation.

SEM

The fractured surface micrographs of the composite samples were taken by using scanning electron microscopy (Quanta 600 SEM). The fractured surface of specimens was made conductive by a sputtered thin layer of gold/palladium alloy in vacuum.

Water uptake Test

The water uptake of the OPF/LLDPE bio-composite was run as stated in the ASTM D570. Disk shaped samples with 50 mm diameter and 3.2 mm thickness, were oven dried at 50°C. Polymer bio-composite specimens were soaked in distilled water at 23 °C for 1 day, then removed, wiped with a paper and weighted.

The water absorption was recorded every day for 30 days, subsequently the water uptake was calculated by using Eqn (2):

$$\text{Water absorption(\%)} = [(W_t - W) / W] \times 100 \quad (2)$$

where, W is the sample dry weight and W_t is the weight of the soaked specimen at any specific time t .

RESULTS AND DISCUSSION

OPF particle size

OPF was obtained using the Pulverisette 9 vibrating cup mill. The ground olive pomace has an average particle size below 200 μm . OPF sample was kept for further inspection.

Density and Moisture Content Measurements of OPF

The bulk density of OPF was measured to be 0.436 g/cm^3 , and the moisture content was 2% for all filler specimens used in the formulated bio-composites material.

Mechanical Characterization of Polymer Bio-composites

Stress and Strain

The tensile stress variation of the OPF/LLDPE polymer bio-composite as a function of the filler loading with and without the Fusabond E226 coupling agent is presented in Figure 1. The mean value of at least seven specimens was measured for each bio-composite formulation.

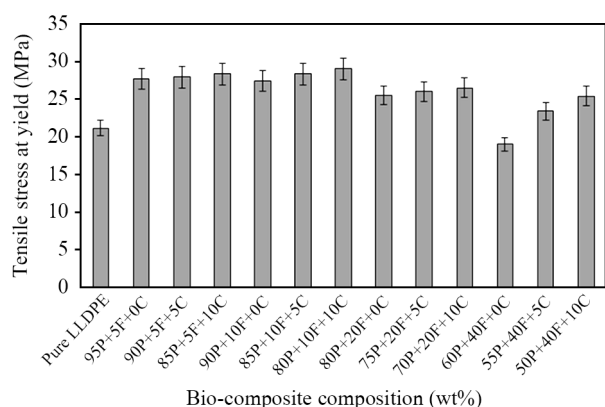


Figure 1. Variation of the tensile stress at yield of the OPF / LLDPE bio-composites with the filler and C content. P: polymer % (LLDPE), F: filler % (OPF) and C: coupling agent % (Fusabond E226).

For the filled polymer bio-composite, 5F, 10F and 20F samples with and without C, the tensile stress at yield increased by 18% compared to that of the neat LLDPE and decreased by 10% at 40F loading level. A marginal drop in the tensile stress at yield was noticed as the filler load increased for 5F, 10F and 20F samples. The tensile stress at yield declined because of the filler high load content (40F) in the LLDPE matrix compared to that of the neat LLDPE. The inferior dispersion of the OPF filler (40F) in the LLDPE matrix had influenced the mechanical properties of the polymer biocomposite compared to that of the neat polymer. The OPF granule size and shape as well as their morphological characteristics are considered to play a role in the obtained mechanical performance [57]. A marginal increase (1% - 2%) in the tensile stress at yield with the increase in the % C was obtained, especially with low to intermediate filler loading contents (5F, 10F, and 20F). On the other hand, the inclusion of C raised the yield tensile stress by 23% and 33% for samples with 40F+5C and 40F+10C, respectively, compared to the uncoupled 40F composite samples. The OPF, originally used without any further chemical treatment, was apt to interrelate with the Fusabond E226 (C), which sequentially enhanced the compatibility of the polymer/filler interface at the higher loading level (40F).

The tensile strain at yield marginally decreased (10%) as the filler loading increased (5%- 40%), as seen in Figure 2. The interfacial adhesion between the hydrophilic lignocelluloses OPF and the hydrophobic LLDPE matrix is apparently compatible due to

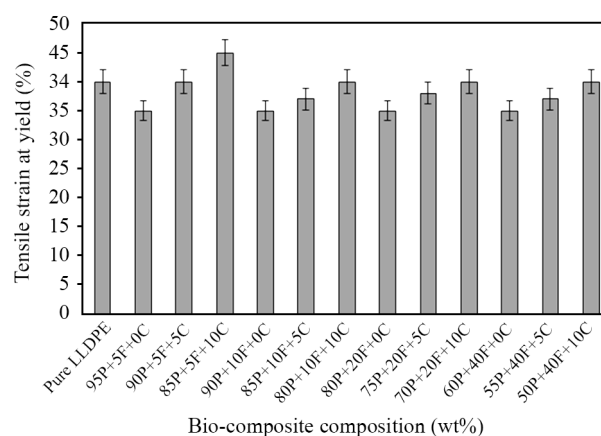


Figure 2. Variation of the tensile strain at yield of the OPF / LLDPE bio-composites with the filler and coupling agent content. P: polymer % (LLDPE), F: filler % (OPF) and C: coupling agent % (Fusabond E226).

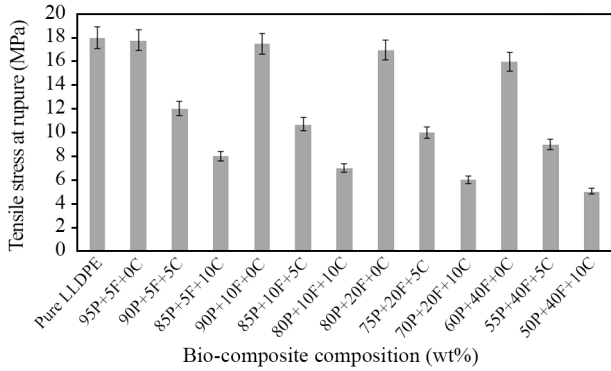


Figure 3. Variation of the tensile stress at rupture of the OPF/LLDPE bio-composites with and without the filler and coupling agent content. P: polymer % (LLDPE), F: filler % (OPF) and C: coupling agent % (Fusabond E226).

the stress transfer between the two phases present in the polymer bio-composite. Fusabond E226 is used to enhance the interfacial adhesion between the OPF and LLDPE polymer bio-composite [58]. C with 5% and 10% contents improved the compatibility between the OPF filler and the LLDPE matrix, therefore improving the bio-composite mechanical properties.

The tensile stress at rupture marginally decreased with the filler content increase for the uncoupled biocomposite samples as shown in Figure 3. Nevertheless, addition of 5% and 10% C to the OPF/LLDPE bio-composite reduced the tensile stress at rupture by 35% and 60 %, respectively. The tensile strain at rupture for the uncoupled polymer bio-composites (5F, 10F, 20F, and 40F) decreased with the OPF content increase by 46%, 53%, 67% and 80%, respectively (Figure 4). Whereas, the addition of 5% and 10% C to the bio-

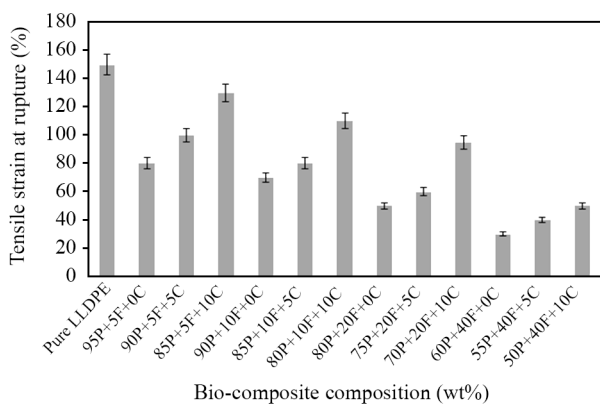


Figure 4. Variation of the tensile strain at rupture of the OPF/LLDPE composites with and without the filler and coupling agent content. P: polymer % (LLDPE), F: filler % (OPF) and C: coupling agent % (Fusabond E226).

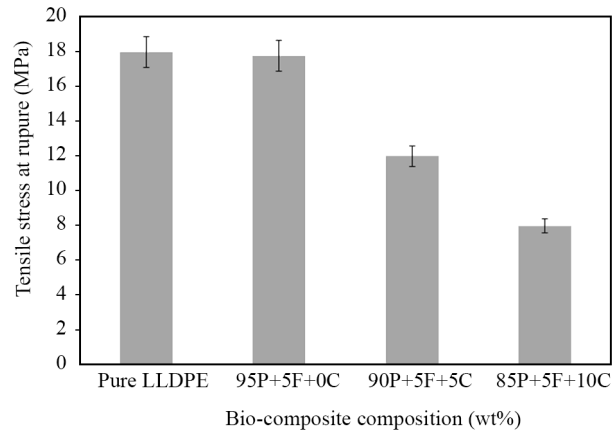


Figure 5. Tensile stress at rupture of the 5% OPF/LLDPE bio-composite as a function of the coupling agent loading. P: polymer % (LLDPE), F: filler % (OPF) and C: coupling agent % (Fusabond E226).

composite material improved the tensile strain at rupture by approximately 20% to 60%, respectively. A decrease in the tensile stress at rupture (Figure 5) and an increase in tensile strain at rupture (Figure 6) in existence of C could be interpreted by the role of softening behavior played by C within the filler/polymer matrix.

Modulus of Elasticity

The tensile modulus of the OPF/LLDPE specimens was evaluated in tensile test. The alteration of the tensile modulus with the OPF content of the bio-composites formulations is shown in Figure 7. The tensile modulus of the uncoupled specimens increased at low filler content (5F, 10F, 20F) followed by a decrease at high level filler loading (40F) which may be attributed to OPF agglomeration phenomenon. The bio-composites

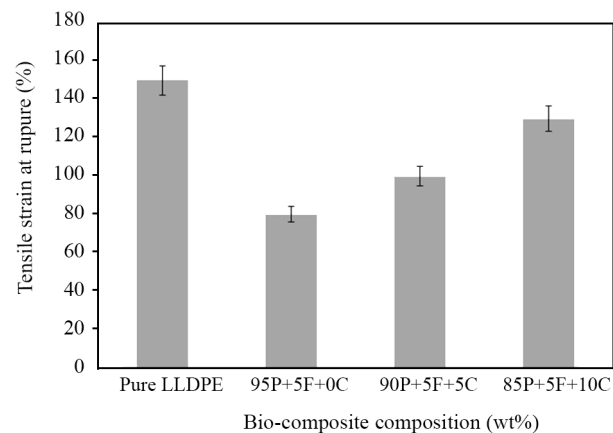


Figure 6. Tensile strain at rupture of the 5% OPF / LLDPE bio-composite as a function of the coupling agent loading. P: polymer % (LLDPE), F: filler % (OPF) and C: coupling agent % (Fusabond E226).

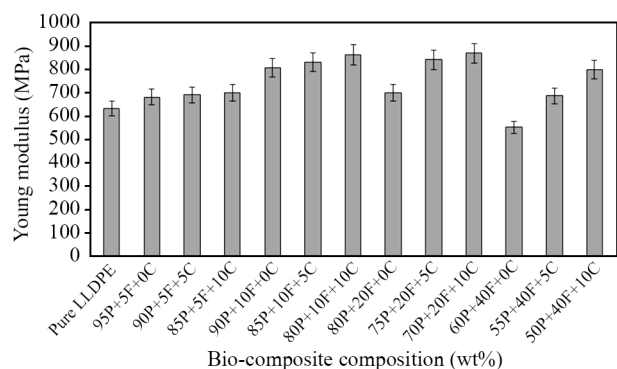


Figure 7. Variation of the tensile modulus of the OPF/LLDPE bio-composites with and without the filler and coupling agent content. P: polymer % (LLDPE), F: filler % (OPF) and C: coupling agent %.

with 5%, 10%, and 20% OPF content have proven a better modulus compared to that of the neat LLDPE. The dispersion nature at low OPF filler content (5%, 10%, and 20% OPF) is the probable cause for the improvement in modulus [59]. For the high filler loading content (40F), the modulus of elasticity decreased by 12% compared to that of the neat polymer. The use of 5% and 10% C did not enhance the modulus of elasticity for low filler content (5F+5C and 5F+10C). The addition of 5% C to bio-composites of higher filler content (10F, 20F, and 40F) boosted the modulus values by 3%, 20%, and 25%, respectively. Whereas, the addition of 10% C to the mentioned filler loading increased the modulus values by 6%, 24%, and 45%, respectively. The addition of Fusabond E226 to the filler /polymer bio-composite seems to play a crucial role in improving the interfacial adhesion of the resulted OPF/LLDPE polymer bio-composite.

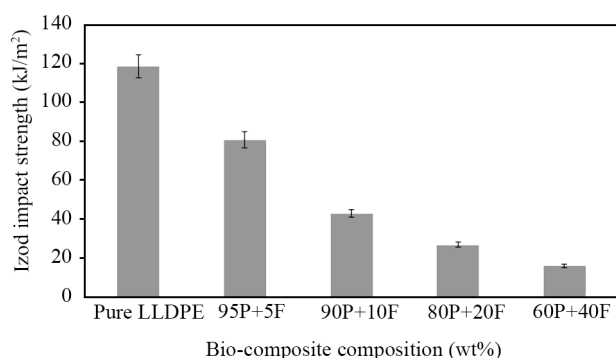


Figure 8. Effect of the OPF content on the impact strength of the OPF/LLDPE composite. P: polymer % (LLDPE), F: filler % (OPF).

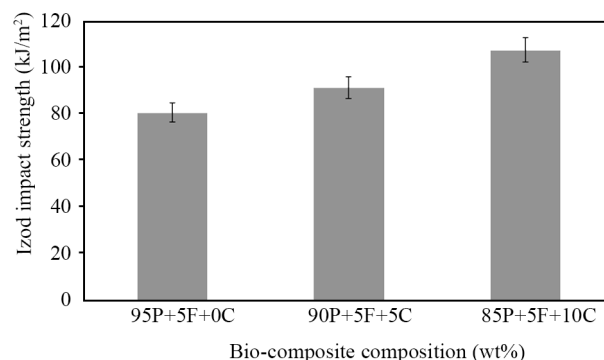


Figure 9. Coupling agent effect on the impact strength of the 5% OPF/LLDPE bio-composite, F: filler % (OPF) and C: coupling agent %.

Izod Impact Strength (un-notched)

The impact strength is the amount of energy necessary to propagate a fracture in material. It depends on particular elements including fiber and matrix strength and other factors such as bonding strength, fiber distribution, and geometry. Figure 8 represents measured values of the impact strengths of the OPF/LLDPE polymer bio-composite.

The un-notched impact resistance of the uncoupled bio-composite samples decreased as the filler loading increased. Moreover, both the energy absorbed by the samples and their toughness decreased. It is observed that the OPF filler loading has an adverse effect on the impact of the OPF/LLDPE bio-composite. Inclusion of the OPF content up to 5%, 10%, 20% and 40% decreased the impact strength of the bio-composites by 32%, 64%, 77%, and 86%, respectively. The addition of the C to the filled polymer matrix improved the impact toughness of the polymer bio-composite due to the coupling effect which interconnected both the filler and polymer phases. The constructive outcome

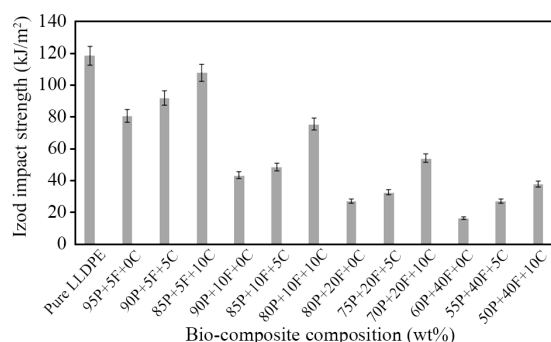


Figure 10. Variation of the impact strength of the OPF/LLDPE bio-composites with and without the filler and coupling agent content. F: filler % (OPF) and C: coupling agent %.

of the C addition on the impact behavior is shown in Figure 9. The addition of 5% and 10% C to 5% OPF/LLDPE bio-composite resulted in an increase in the impact strength on the order of 12% and 34%, respectively [60].

The collective impact strength behavior of the various filler and C percentages of the different OPF/LLDPE bio-composite formulations is summarized in Figure 10. The impact strength showed both a decrease and an increase trend upon increasing the percent of the filler and of the C, respectively. The poor filler dispersion resulted in the formation of the agglomerates which may induce non-uniform stress transfer thus decrease the impact strength of the polymer bio-composite on the filler addition [61, 62]. Whereas, the addition of the C reduced the possibility of the filler particles agglomerates and enhanced the impact strength of the coupled OPF/LLDPE bio-composite samples [63].

Fractured Surface Morphology

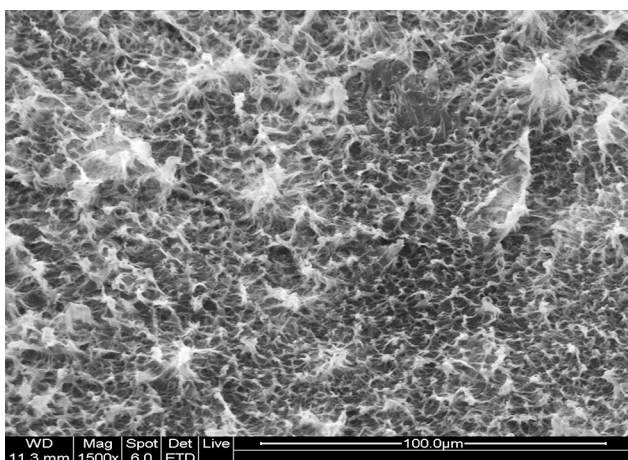
The OPF filler used has an irregular particle shape with a particle size below 200 μm . The fractured surfaces of the neat LLDPE polymer and the filled polymer bio-composites were examined with SEM. Fractured surface of the neat LLDPE with 1500x and 4000x magnifications are shown in Figure 11 with homogeneous polymer surface and well-defined morphologies.

The morphology of the OPF/LLDPE bio-composite (Figure 12) is slightly different from that of the neat LLDPE. When the OPF loading level increased from

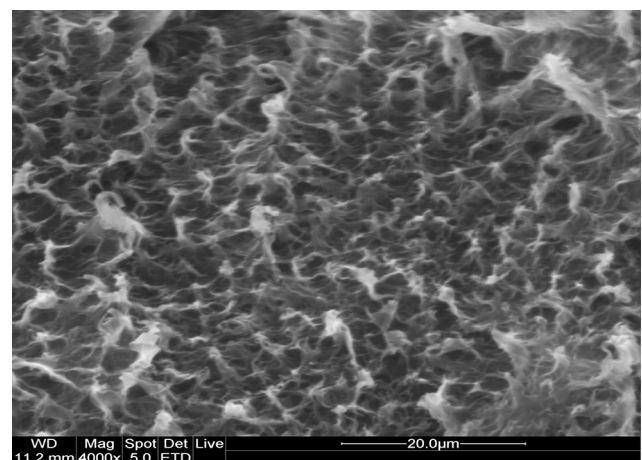
10% to 40% as shown in Figure 12 (B, C, D), the polymer bio-composite matrix pullout was decreased, respectively. The weak interfacial adhesion between the polymer and filler interfaces upon increasing filler loading level was noticed. The presence of both empty cavities and filled spaces within the polymer bio-composite is clear and showed an ease in debonding during the fracture process. The less pullout in the polymer bio-composite fractured surface upon increasing filler loading level is in good agreement with the inferior tensile behavior when compared to that of unfilled LLDPE polymer [64].

The interfacial adhesion between the OPF and LLDPE polymer matrix was enhanced by using 5% and 10% C. The addition of 5% C to 5% OPF-filled polymer bio-composite is shown in Figure 13. Various modifications at (A: 95x, B: 534x, C: 2252x, and D: 5242x) were used to shed light on the development of interfacial adhesion between the neat LLDPE polymer and the OPF filler in the polymer bio-composite matrix. An oval predominant OPF filler shape was found in the polymer bio-composite matrix. Figure 13 C shows the interfacial adhesion between the polymer and filler interface. The phase morphology changes upon 5% C addition is in a good agreement with the increase in the impact strength and the strain at rupture of the polymer bio-composite.

The inclusion of 10% C to 5% OPF-filled LLDPE polymer bio-composite is shown in Figure 14 at various magnification levels (A:136x, B: 542x, C: 2393x, and D: 3829x). The development of C effect on the inter-



(a)



(b)

Figure 11. SEM of the fractured surfaces of the neat LLDPE at 1500x and 4000x magnifications.

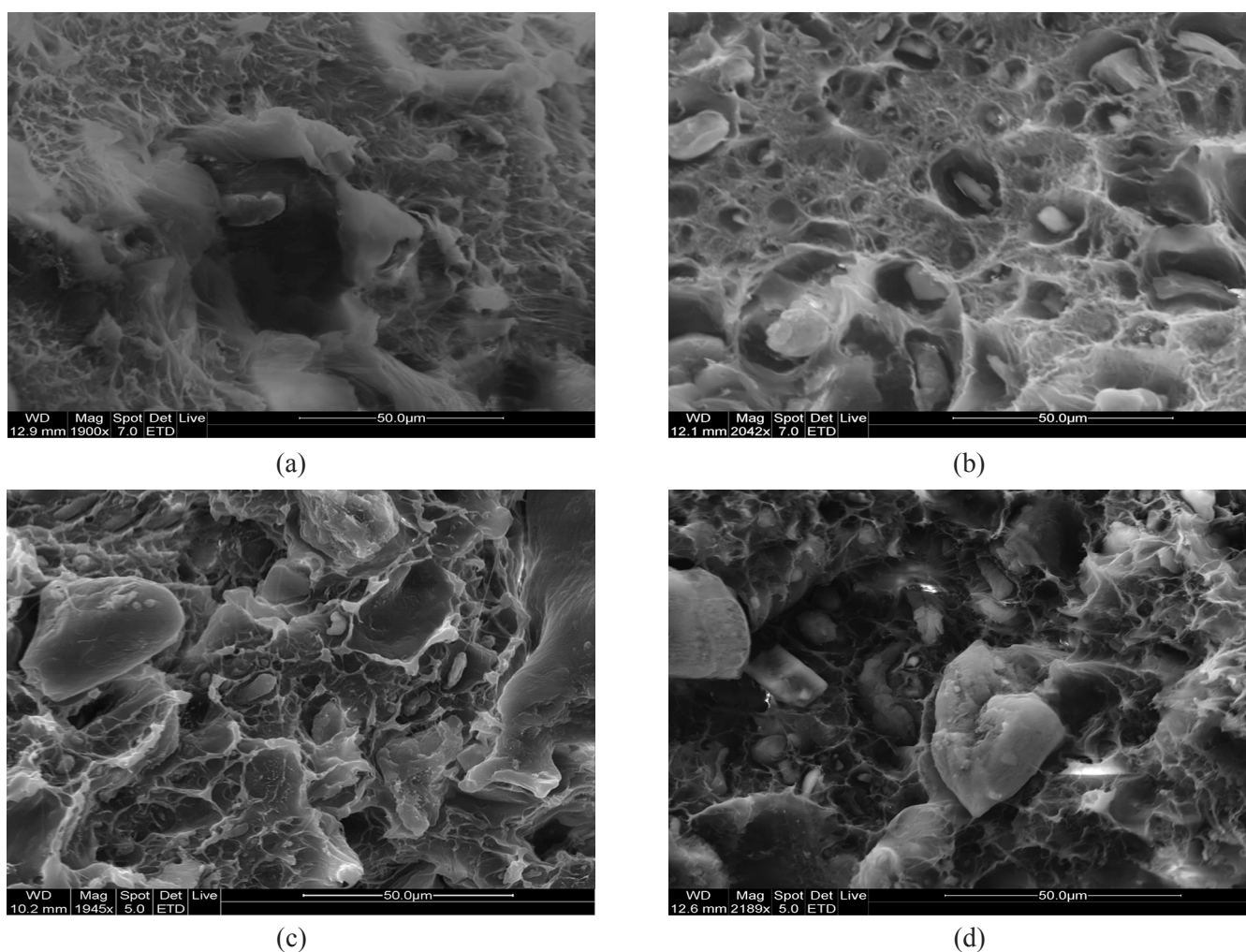


Figure 12. SEM of the fractured surfaces of the OPF/LLDPE bio-composite at various filler loading levels (a) 5, (b) 10, (c) 20, and (d) 40 wt. %.

facial adhesion is clearly shown in Figure 14 (C, D), where polymer flow veins adhere well to the surface of the OPF filler. Polymer bio-composite pullout behavior at this point is in good matching with the increase in strain at rupture and the impact strength data presented in previous stress-strain mechanical behavior of the present polymer bio-composite.

The interfacial adhesion between the filler/polymer phases was improved upon the addition of C, which crucially decreased the tension at the material interface, and thus, allowed the formation of the compatible composite phase boundaries that finally affected the mechanical properties of the polymer bio-composite. Good surrounding and sticking of the OPF filler to the LLDPE polymer matrix caused enhancement of the strain at rupture and the impact strength compared with those of the uncoupled polymer bio-composites [65].

Water Absorption

Composites formulated using wood fillers are normally susceptible to water. The mechanical performance of the wood composites is unfavorably affected by water surroundings. The apolar nature and low interfacial adherence of the filler to the polymer reduce the mechanical performance of the polymer composite. The water uptake % as a function of the contact time at varying OPF and C loadings is apparent in Figure 15. The water uptake % raised slightly and gradually and then slowed down after about 25 days of immersion in water environment.

The usage of the OPF in polyolefin matrix LLDPE increased water absorption as demonstrated in Figure 15. Water uptake % decreased with the addition of C to polymer bio-composite due to the decrease in hydrophilic nature of the lignocellulosic content of the composite material [66]. Bio-composites with C of 5%

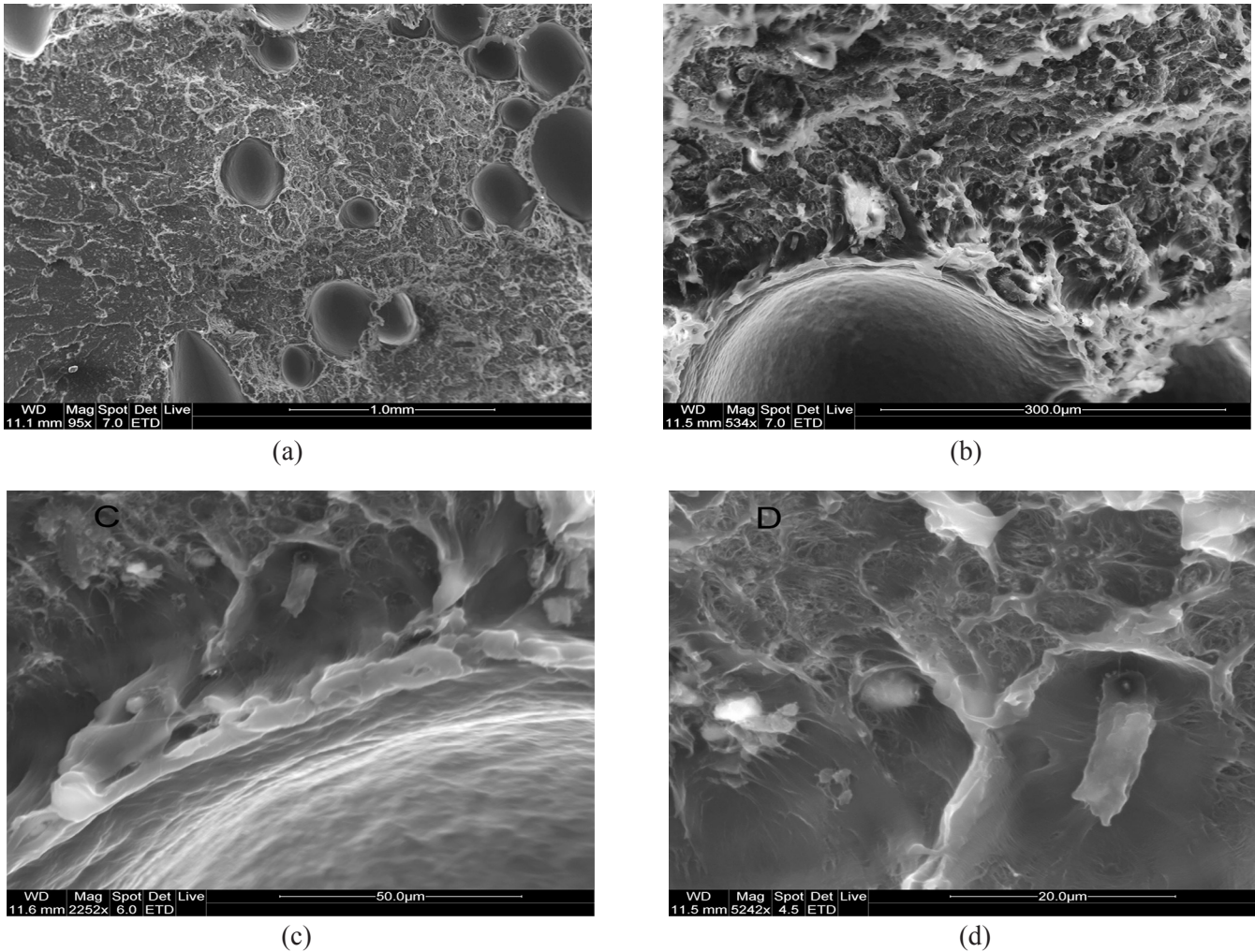


Figure 13. SEM of the fractured surfaces of the OPF / LLDPE bio-composite with 5% OPF and 5% C at different magnifications (a) 95x, (b) 534x, (c) 2252x, and (d) 5242x.

(■) and 10% (▲) demonstrated a decline in the water uptake from about 38% to 52%, respectively, when compared to the uncoupled polymer bio-composites (●). The presence of C in the polymer bio-composite resulted in better interfacial adhesion between the two phases of LLDPE polymer and OPF filler. As a result, water sensitivity of the polymer bio-composite reduced with the C inclusion.

CONCLUSIONS

Bio-composite material containing OPF spread in the LLDPE matrix was formulated and investigated. The effect of the OPF at various loading levels with and without using C was investigated. Mechanical, morphological, and water uptake properties of OPF-filled LLDPE bio-composite are discussed herein. The OPF/

LLDPE bio-composites with 5, 10, 20, and 40 wt.% OPF were mixed and processed in an extruder and a hot press machine. Manufacturing of the LLDPE bio-composites with certain OPF loading level was performed in a single stage extrusion process where the OPF, C, and LLDPE are directly delivered into the extruder. The variation of the filler and C loading levels resulted in varying properties of the product. For bio-composites, tensile stress at yield increased by 20% and the stress at rupture decreased by 20%, showed competitive tensile stress values compared to that of the neat LLDPE and of the uncoupled low filled polymer samples (<40% F). The addition of C to OPF-filled polymer resulted in decreasing the tensile stress at rupture and increasing the tensile strain at rupture. Young's modulus of the bio-composites less than 40 % OPF increased upon inclusion of both filler and C. Impact strength of the OPF/LLDPE bio-composite decreased

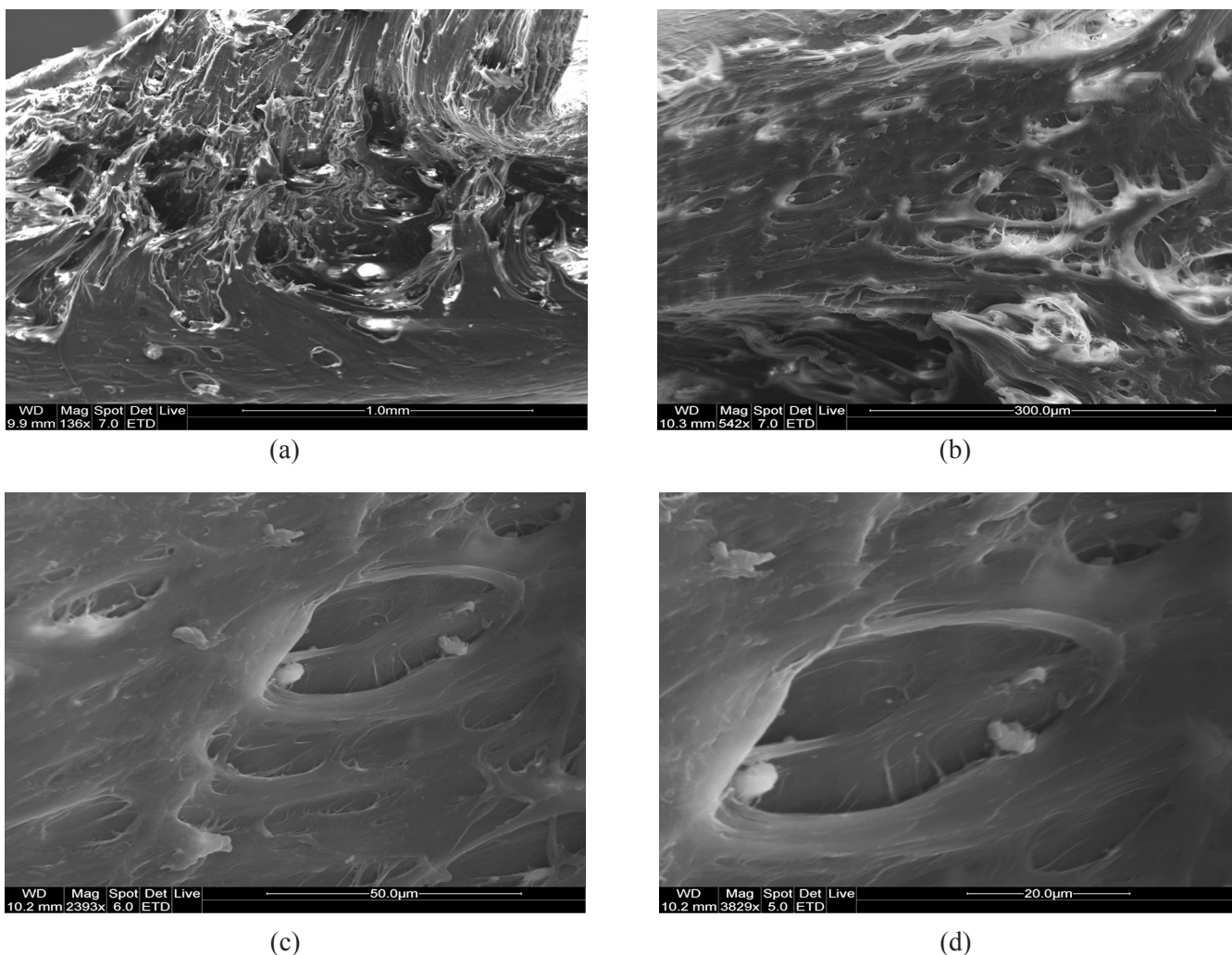


Figure 14. SEM of the fractured surfaces of the OPF/LLDPE bio-composite with 5% OPF and 10% C at different magnifications (a) 136x, (b) 542x, (c) 2393x, and (d) 3829x.

with the filler loading and increased with the C addition. The OPF/LLDPE poor phase compatibility is a real challenge in introducing a competitive polymer bio-composite with acceptable mechanical performance. Morphologically, the polymer bio-composite samples showed the necessity of using C to reduce the interfacial surface tension and to enhance the compatibility between the two different phase boundaries. The decrease in mechanical performance could be stopped and improved on using proportional quantities of C. Water uptake raised with filler loading and diminished on addition of C which is in good agreement with mechanical performance outputs. Poor interfacial adhesion between the cellulosic fillers and non-polar olefin polymers is the main obstacle in producing mechanically competitive bio-composite material. Efforts to overcome such a problem have

been partially met for some filler/polymer matrices, yet improvement in decreasing interfacial surface tension

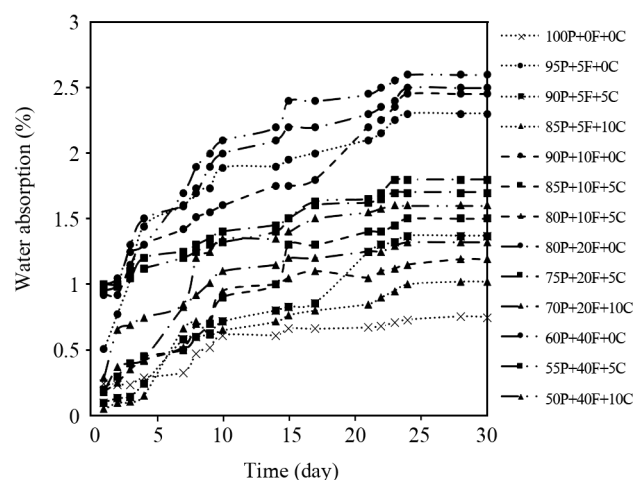


Figure 15. Water absorption of the OPF / LLDPE bio-composite vs. time.

between incompatible phases needs more investigation.

ACKNOWLEDGEMENTS

Authors would like to express their gratitude to Al al-Bayt University for support throughout this work.

CONFLICTS OF INTEREST

The authors declare that they have no conflicts of interest.

REFERENCES

1. Thakur KT, Rana AK, Thakur VK (2014) Lignocellulosic Polymer composites: A brief overview. In: Lignocellulosic polymer composites: Processing, characterization, and properties, Ed: Thakur VK, Wiley online library, 1-15
2. Thakur VK, Kessler MR (2016) Green biorenewable biocomposites: From knowledge to industrial applications, CRC Press
3. Lima MA, Gomez LD, Steele-King CG, Simister R, Bernardinelli OD, Carvalho MA, Rezende CA, Labate CA, Eduardo RD, McQueen-Mason SJ, Polikarpov I (2014) Evaluating the composition and processing potential of novel sources of Brazilian biomass for sustainable biorenewables production. *Biotech Biofuels* 7: 10
4. Maya JJ, Sabu T (2008) Biofibres and biocomposites. *Carbohydr Polym* 71: 343-364
5. Puglia D, Biagiotti J, Kenny JM (2005) A review on natural fibre-based composites-Part II: Application of natural reinforcements in composite materials for automotive industry. *J Nat fibers* 1: 23-65
6. Gupta MK, Srivastava RK (2016) Mechanical properties of hybrid fibers-reinforced polymer composite: A review. *Polym Plast Technol Eng* 55: 626-642
7. Kaya N, Atagur M, Akyuz O, Seki Y, Sarikanat ME, Sutcu M, Seydibeyoglu MO, Sever K (2018) Fabrication and characterization of olive pomace filled PP composites. *Compos Part B-Eng* 150: 277-283
8. Boudria A, Hammoui Y, Adjeroud N, Djerrada N, Madani K (2018) Effect of filler load and high-energy ball milling process on properties of plasticized wheat gluten/olive pomace biocomposite. *Adv Powder Technol* 29: 1230-1238
9. Lammi S, Barakat A, Mayer-Laigle C, Djenane D, Gontard N, Angellier-Coussy H (2018) Dry fractionation of olive pomace as a sustainable process to produce fillers for biocomposites. *Powder Technol* 326: 44-53
10. Kuciel S, Jakubowska P, Kuźniar P (2014) A study on the mechanical properties and the influence of water uptake and temperature on biocomposites based on polyethylene from renewable sources. *Compos Part B-Eng* 64: 72-77
11. Réquillé S, Le Duigou A, Bourmaud A, Baley C (2019) Deeper insights into the moisture-induced hygroscopic and mechanical properties of hemp reinforced biocomposites. *Compos Part A-Appl S* 123: 278-285
12. Halimatul MJ, Sapuan SM, Jawaid M, Ishak MR, Ilyas RA (2019) Water absorption and water solubility properties of sago starch biopolymer composite films filled with sugar palm particles. *Polimery* 64: 596-604
13. Sullins T, Pillay S, Komus A, Ning H (2017) Hemp fiber reinforced polypropylene composites: The effects of material treatments. *Compos Part B-Eng* 114: 15-22
14. Guna V, Ilangovan M, Rather MH, Giridharan BV, Prajwal B, Krishna KV, Venkatesh K, Reddy N (2020) Groundnut shell/rice husk agro-waste reinforced polypropylene hybrid biocomposites. *J Build Eng* 27: 100991
15. Zhang J, Wang R, Liu H, Wu H, Wu T, Wu Z, Xiang W, Wen S, Cai X (2020) Effect of artemisia argyi charcoal on the mechanical property and thermal stability of polypropylene. *Plast Rubber Compos* 7: 1-7
16. Valdivia M, Galan JL, Laffarga J, Ramos JL (2016) Biofuels 2020: Biorefineries based on lignocellulosic materials. *Microb Biotechnol* 9: 585-594
17. Bowyer JL, Stockmann VE (2001) Agricultural

- residues. *Forest Prod J* 51: 10-21
18. Mohanty AK, Misra M, Drzal LT (2002) Sustainable bio-composites from renewable resources: opportunities and challenges in the green materials world. *J Polym Environ* 10: 19-26
 19. Yusuf AA, Inambao FL (2020) Characterization of Ugandan biomass wastes as the potential candidates towards bioenergy production. *Renew Sustain Energy Rev* 117: 109477
 20. Parveen N, Singh DV, Azam R (2020) Innovations in recycling for sustainable management of solid wastes. In: *Innovative waste management technologies for sustainable development*, IGI Global, 177-210
 21. Gholampour A, Ozbakkaloglu T (2020) A review of natural fiber composites: Properties, modification and processing techniques, characterization, applications. *J Mater Sci* 1: 1-64
 22. Tasdemir M (2017) Effects of olive pit and almond shell powder on polypropylene. In: *Key engineering materials*. Trans Tech Publications Ltd, 733: 65-68
 23. Jawaid M, Tahir PM, Saba N (2017) Lignocellulosic fibre and biomass-based composite materials: Processing, properties and applications. Woodhead Publishing
 24. Elshahli E, Elhrari W, Klash A, Shebani A (2016) The use of olive stone waste for production of particleboard using commercial polyster sealer as a binding agent. In: *1st International Conference on Chemical, Petroleum, and Gas Engineering (ICCPGE 2016)*
 25. Gowman AC, Picard MC, Lim LT, Misra M, Mohanty AK (2019) Fruit waste valorization for biodegradable biocomposite applications: A review. *Bio Resources* 14: 10047-10092
 26. Maksimović M, Omanović-Miklićanin E (2017) Towards green nanotechnology: Maximizing benefits and minimizing harm. In: *CMBEBIH*, Springer, Singapore, 164-170
 27. Horodytska O, Valdés FJ, Fullana A (2018) Plastic flexible films waste management—A state of art review. *J Waste Manag* 77: 413-425
 28. Wu J, Du X, Yin Z, Xu S, Xu S, Zhang Y (2019) Preparation and characterization of cellulose nanofibrils from coconut coir fibers and their reinforcements in biodegradable composite films. *Carbohydr polym* 211:49-56
 29. Hassan MM, Le Guen MJ, Tucker N, Parker K (2019) Thermo-mechanical, morphological and water absorption properties of thermoplastic starch/cellulose composite foams reinforced with PLA. *Cellulose* 26: 4463-4478
 30. Khodaeimehr R, Peighambaroust SJ, Peighambaroust SH (2018) Preparation and characterization of corn starch/clay nanocomposite films: Effect of clay content and surface modification. *Starch-Stärke* 70: 1700251
 31. Hajizadeh H, Peighambaroust SJ, Peighambaroust SH, Peressini D (2020) Physical, mechanical, and antibacterial characteristics of bio-nanocomposite films loaded with Ag-modified SiO₂ and TiO₂ nanoparticles. *J Food Sci* 85: 1193-1202
 32. Peighambaroust SJ, Peighambaroust SH, Pournasir N, Pakdel PM (2019) Properties of active starch-based films incorporating a combination of Ag, ZnO and CuO nanoparticles for potential use in food packaging applications. *Food Packag Shelf Life* 22: 100420
 33. Dehghani S, Peighambaroust SH, Peighambaroust SJ, Hosseini SV, Regenstein JM (2019) Improved mechanical and antibacterial properties of active LDPE films prepared with combination of Ag, ZnO and CuO nanoparticles. *Food Packag Shelf Life* 22: 100391
 34. Ebrahimi Y, Peighambaroust SJ, Peighambaroust SH, Karkaj SZ (2019) Development of antibacterial carboxymethyl cellulose-based nanobiocomposite films containing various metallic nanoparticles for food packaging applications. *J Food Sci* 84: 2537-2548
 35. Azwa ZN, Yousif BF, Manalo AC, Karunasena W (2013) A review on the degradability of polymeric composites based on natural fibres. *Mater Design* 47: 424-442
 36. John MJ, Thomas S (2008) Biofibres and biocomposites. *Carbohydr polym* 71: 343-364
 37. Kaya N, Atagur M, Akyuz O, Seki Y, Sarikanat ME, Sutcu M, Seydibeyoglu MO, Sever K (2018) Fabrication and characterization of olive pomace filled PP composites. *Compos Part B-Eng* 150:

- 277-283
38. Lammi S, Le Moigne N, Djenane D, Gontard N, Angellier-Coussy H (2018) Dry fractionation of olive pomace for the development of food packaging biocomposites. *Ind crops prod* 120: 250-261
 39. Gharbi A, Hassen RB, Boufi S (2014) Composite materials from unsaturated polyester resin and olive nuts residue: the effect of silane treatment. *Ind Crops Prod* 62: 491-498
 40. Banat R (2019) Olive pomace flour as potential organic filler in composite materials: A brief review. *Am J Polym Sci* 9: 10-15
 41. Koutsomitopoulou AF, Bénézet JC, Bergeret A, Papanicolaou GC (2014) Preparation and characterization of olive pit powder as a filler to PLA-matrix bio-composites. *Powder Technol* 255: 10-16
 42. Perinović S, Andričić B, Kovačić T, Vučenović V (2008) Influence of citric plasticizers on thermal properties of poly (l-lactide)/olive stone flour composites. In: *International Conference MATRIB 2008*
 43. Perinović S, Andričić B (2012) Modification of properties of poly (L-lactide). *Polimeri: časopis za plastiku i gumu*. 33: 100-105
 44. Naghmouchi I, Espinach FX, Mutjé P, Boufi S (2015) Polypropylene composites based on lignocellulosic fillers: How the filler morphology affects the composite properties. *Mater Design* 65: 454-461
 45. Siracusa G, La Rosa AD, Siracusa V, Trovato M (2001) Eco-compatible use of olive husk as filler in thermoplastic composites. *J Polym Environ* 9: 157-161
 46. Amar B, Salem K, Hocine D, Chadia I, Juan MJ (2011) Study and characterization of composites materials based on polypropylene loaded with olive husk flour. *J Appl Polym Sci* 122: 1382-1394
 47. Naghmouchi I, Mutjé P, Boufi S (2014) Polyvinyl chloride composites filled with olive stone flour: mechanical, thermal, and water absorption properties. *J Appl Polym Sci* 131: 41083
 48. Tserki V, Matzinos P, Panayiotou C (2006) Novel biodegradable composites based on treated lignocellulosic waste flour as filler. Part II. Development of biodegradable composites using treated and compatibilized waste flour. *Compos Part-A Appl S* 37: 1231-1238
 49. Lammi S, Le Moigne N, Djenane D, Gontard N, Angellier-Coussy H (2018) Dry fractionation of olive pomace for the development of food packaging biocomposites. *Ind Crops Prod* 120: 250-61
 50. Lammi S, Barakat A, Mayer-Laigle C, Djenane D, Gontard N, Angellier-Coussy H (2018) Dry fractionation of olive pomace as a sustainable process to produce fillers for biocomposites. *Powder Technol* 326: 44-53
 51. Gharbi A, Hassen RB, Boufi S (2014) Composite materials from unsaturated polyester resin and olive nuts residue: the effect of silane treatment. *Ind Crops Prod* 62: 491-498
 52. Papanicolaou GC, Koutsomitopoulou AF, Sfakianakis A (2012) Effect of thermal fatigue on the mechanical properties of epoxy matrix composites reinforced with olive pits powder. *J Appl Polym Sci* 124: 67-76
 53. Papanicolaou GC, Xepapadaki AG, Angelakopoulos GC, Zabaniotou A, Ioannidou O (2011) Use of solid residue from olive kernel pyrolysis for polymer matrix composite manufacturing: Physical and mechanical characterization. *J Appl Polym Sci* 19: 2167-2173
 54. Abou-Zeid RE, Hassan EA, Bettaieb F, Khiari R, Hassan ML (2015) Use of cellulose and oxidized cellulose nanocrystals from olive stones in chitosan bionanocomposites. *J Nanomater* 2015: 687490
 55. Pereda M, Dufresne A, Aranguren MI, Marcovich NE (2014) Polyelectrolyte films based on chitosan/olive oil and reinforced with cellulose nanocrystals. *Carbohydr Polym* 101: 1018-1026
 56. Hammoui Y, Molina-Boisseau S, Duval A, Djerrada N, Adjeroud N, Remini H, Dahmoune F, Madani K (2015) Preparation of plasticized wheat gluten/olive pomace powder biocomposite: Effect of powder content and chemical modifications. *Mater Design* 87: 742-749
 57. Fu SY, Feng X Q, Lauke B, and Mai YW (2008) Effects of particle size, particle/matrix interface adhesion and particle loading on mechanical

- properties of particulate–polymer composites. *Compos Part B-Eng* 39: 933-961
58. Tian H, Yao Y, Liu D, Li Y, Jv R, Xiang G and Xiang A (2019) Enhanced interfacial adhesion and properties of polypropylene/carbon fiber composites by fiber surface oxidation in presence of a compatibilizer. *Polym Compos* 40(S1): E654-E662
 59. Ishak WHW, Rosli NA and Ahmad I (2020) Influence of amorphous cellulose on mechanical, thermal, and hydrolytic degradation of poly (lactic acid) biocomposites. *Sci Rep* 10: 1-13
 60. Bledzki AK, & Faruk O (2003) Wood fibre reinforced polypropylene composites: Effect of fibre geometry and coupling agent on physico-mechanical properties. *Applied Composite Materials* 10: 365-379
 61. Thomason JL, Rudeiros-Fernández JL (2018) A review of the impact performance of natural fiber thermoplastic composites. *Front Mater* 5: 60
 62. Dehbari N, Moazeni N, Wan Abdul Rahman WA (2014) Effects of kenaf core on properties of poly (lactic acid) bio-composite. *Polym Compos* 35: 1220-1227
 63. He S, Xue Y, Lin J, Zhang L, Du X, Chen L (2016) Effect of silane coupling agent on the structure and mechanical properties of nano-dispersed clay filled styrene butadiene rubber. *Polym Compos* 37: 890-896
 64. Marcovich NE, Villar MA (2003) Thermal and mechanical characterization of linear low-density polyethylene/wood flour composites. *J Appl Polym Sci* 90: 2775-2784
 65. Anbupalani MS, Venkatachalam CD, Rathanasamy R (2020) Influence of coupling agent on altering the reinforcing efficiency of natural fibre-incorporated polymers—a review. *J Reinf Plast Compos* 39: 520-544
 66. Dolza C, Fages E, Gongga E, Gomez-Caturla J, Balart R, Quiles-Carrillo L (2021) Development and characterization of environmentally friendly wood plastic composites from biobased polyethylene and short natural fibers processed by injection moulding. *Polymers* 13: 1692